



## Development of magnetically retrievable spinel nanoferrites as efficient catalysts for aminolysis of epoxides with amines

Ankush Sheoran<sup>a</sup>, Manisha Dhiman<sup>a</sup>, Santosh Bhukal<sup>b</sup>, Rupal Malik<sup>a</sup>, Jyoti Agarwal<sup>a</sup>, Bhupendra Chudasama<sup>c</sup>, Sonal Singhal<sup>a,\*</sup>

<sup>a</sup> Department of Chemistry, Panjab University, Chandigarh, 160014, India

<sup>b</sup> Guru Jambheshwar University of Science and Technology, Hisar, 125001, India

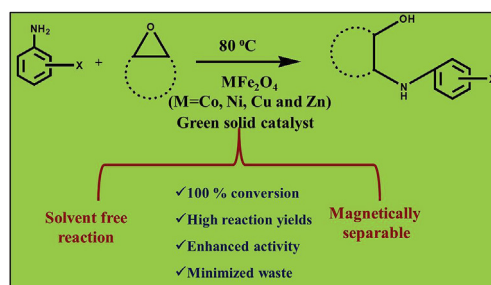
<sup>c</sup> School of Physics & Materials Science, Thapar University, Patiala, 147004, India

### HIGHLIGHTS

- Spinel nano ferrites (M = Co, Ni, Cu and Zn) were successfully fabricated by different techniques.
- All the nanoferrites possessed small particle size, high surface area and good magnetic character.
- Catalytic activity was tested for epoxide ring opening reaction under solvent free conditions.
- CoFe<sub>2</sub>O<sub>4</sub> nanoparticles synthesized hydrothermally were found to exhibit maximum activity.

### GRAPHICAL ABSTRACT

Magnetically separable spinel nanoferrites as proficient green catalysts for epoxide ring opening reactions under solvent free conditions.



### ARTICLE INFO

#### Keywords:

Magnetic nanoferrites  
Heterogeneous catalysis  
Epoxide ring opening  
Green chemistry

### ABSTRACT

Magnetically separable spinel nanoferrites (MFe<sub>2</sub>O<sub>4</sub>; M = Co, Ni, Cu and Zn) have been used as proficient catalysts for epoxide ring opening with amines. To study the effect of synthetic methodology on the catalytic activity, all the spinel nanoferrites were fabricated using three different techniques i.e sol-gel, hydrothermal and micro-emulsion method. The synthesized samples exhibited small particle size and high surface area values along with sufficiently magnetic nature to be used as magnetically separable heterogeneous green catalysts. The commencement of the important epoxide ring opening reaction via a green approach i.e by using magnetically recyclable nanoferrites under solvent free conditions in a very short reaction time (4–25 min), is the main highlight of the present work. Best catalytic results for epoxide ring opening were obtained with CoFe<sub>2</sub>O<sub>4</sub> nanoparticles prepared using hydrothermal method which resulted in 100% conversion of the reactants to the corresponding amino alcohol.

### 1. Introduction

In recent years, green chemistry has gained great importance for the design of chemical processes that utilize environment friendly conditions to reduce or eliminate the generation of hazardous substances.

Green chemistry involves various processes that can be potted as safer synthesis, safer products, renewable sources, catalysis, waste prevention, energy efficiency, degradability, pollution control and accident prevention [1]. The exploitation of solvent free reactions represents a unified effort towards the green chemical approach which not only

\* Corresponding author.

E-mail addresses: [sonal@pu.ac.in](mailto:sonal@pu.ac.in), [sonal1174@gmail.com](mailto:sonal1174@gmail.com) (S. Singhal).

<https://doi.org/10.1016/j.matchemphys.2018.10.021>

Received 29 June 2018; Received in revised form 31 July 2018; Accepted 8 October 2018

Available online 10 October 2018

0254-0584/ © 2018 Elsevier B.V. All rights reserved.

solves the economic problems, but also reduces the burden of solvent disposal. Another greener feature involves the use of environmentally benign and recyclable magnetic nanocatalysts, which possess advantages such as low preparation cost, high activity, great selectivity, high stability, efficient recovery and good recyclability [2,3]. The major advantage of using magnetic nanocatalysts is their easy magnetic separation that prevents the loss of catalyst and enhances reusability.

Spinel ferrites are one such class of magnetic nanomaterials which have attracted a great deal of attention in the field of catalysis due to various interesting features such as smaller particle size, high stability, moderate saturation magnetization, easy separation and good recyclability [4–6]. Further, the structural flexibility of spinel ferrites allows easy modifications in their catalytic properties. The catalytic properties of spinel ferrites are greatly affected by change in the synthetic procedure. Various synthetic procedures such as sol-gel route [7], hydrothermal method [8], microemulsion technique [9], ball-mill method [10] have been employed by various researchers in order to change the particle size, morphology and overall the catalytic activity of the spinel ferrites. Various authors have reported the use of spinel ferrites as the catalysts in different organic reactions. Moghaddam et al. [11] have reported the synthesis of spinel ferrites ( $MFe_2O_4$ ;  $M = Ni, Cu$  and  $Co$ ) using co-precipitation method and compared their catalytic activities for the  $\alpha$ -arylation of oxindole derivatives under the optimized reaction conditions. The catalysts allowed the  $\alpha$ -arylation of different types of oxindole derivatives under mild conditions in very good yields and short reaction times. Jadhav et al. [12] have reported the synthesis of mesoporous zinc ferrite nanoparticles via co-precipitation method. The synthesized nanoparticles were then used for the synthesis of nopol by Prins condensation of  $\beta$ -pinene and para formaldehyde. The catalyst resulted in 70% conversion of  $\beta$ -pinene to nopol with 88% selectivity. The nanocatalyst was also found to be active towards other commercially important reactions such as isomerization, acetalization and aldol condensation. Sarode et al. [13] have reported the synthesis of copper ferrite nanoparticles via co-precipitation and thermal decomposition method. The nanoparticles were then used for the synthesis of 2-substituted benzoxazole by using one pot redox cascade condensation reaction of benzyl amine and 2-nitro phenol. The catalyst was reported to be highly active, air stable and recyclable upto six catalytic runs without any significant loss in activity.

Epoxide ring opening (ERO) is a very useful reaction as it offers a suitable route for the formation of C-C, C-N, C-S or C-O bonds. ERO is one of the key steps to synthesize polyketide skeleton, which are one of the most important organic intermediates for the synthesis of various organic compounds [14]. Though numerous reports are published for the epoxide ring opening using homogenous catalysts, very few reports are available for the epoxide ring opening using heterogeneous catalysts such as amberlyst-15 [15], heteropolyacid [16], zeolites [17],  $BiCl_3$  [18], MCM-22 [19] and silica nanoparticles [20] etc. Hence, it is of great importance to develop such a heterogeneous catalyst, which can work in environment friendly conditions and also possess features such as facile magnetic separation and recyclability. Keeping in mind the advantages of spinel ferrites, the present work deals with the epoxide ring opening using spinel ferrites ( $MFe_2O_4$ ;  $M = Co, Ni$  and  $Zn$ ). Also, to study the effect of synthetic procedures on the catalytic properties of the catalysts, all the three ferrites have been synthesized using three different methodologies viz. sol-gel route, hydrothermal method and microemulsion technique. Keeping in mind the green chemistry approach, all the reactions have been performed under solvent free conditions at room temperature.

## 2. Experimental

### 2.1. Materials

Cobalt nitrate hexahydrate ( $Co(NO_3)_2 \cdot 6H_2O$ ), ferric nitrate ( $Fe(NO_3)_3 \cdot 9H_2O$ ), nickel nitrate ( $Ni(NO_3)_2 \cdot 6H_2O$ ), zinc nitrate ( $Zn$

$(NO_3)_2 \cdot 6H_2O$ ), copper nitrate ( $Cu(NO_3)_2 \cdot 3H_2O$ ), sodium dodecyl sulfate (SDS) and sodium hydroxide (NaOH) were purchased from CDH chemicals. AR grade 1-Butanol, ethylene glycol and hexane were purchased from Avra chemicals and citric acid ( $C_6H_8O_7$ ) was purchased from Fisher Scientific. All the obtained chemicals were then used as such without any further purification. Distilled water was obtained using an ultra-filtration system (Milli-Q, Milipore).

### 2.2. Synthesis processes

To study the effect of synthetic methodology on the catalytic properties, all the four metal ferrites ( $MFe_2O_4$ ;  $M = Co, Ni, Cu$  and  $Zn$ ) were fabricated using three different techniques i.e sol-gel method, hydrothermal technique and microemulsion route. The detailed synthetic procedure for the synthesis of spinel nanoferrites using different techniques is discussed below.

#### 2.2.1. Synthesis of $MFe_2O_4$ via sol-gel approach

All the spinel nanoferrites ( $MFe_2O_4$ ;  $M = Co, Ni, Cu$  and  $Zn$ ) were prepared by dissolving metal salt, ferric nitrate and citric acid separately in minimum amount of deionized water in 1:1 M ratio. The solutions were thoroughly mixed and dissolved with continuous stirring and heating at about 80–90 °C. After that citric acid solution was added to the reaction mixture followed by addition of ethylene glycol (10 mL) to initiate gel formation. Resulting gels were dried and crushed to get ferrite powder [21]. The acquired ferrite powders were then subjected to annealing in a silica crucible for 2 h at 400 °C to acquire crystalline ferrites.

#### 2.2.2. Synthesis of $MFe_2O_4$ via hydrothermal approach

In the hydrothermal method, all the spinel nanoferrites were prepared by dissolving the stoichiometric amounts of metal salt and ferric nitrate in minimum amount of distilled water. The pH of the solution was adjusted at 7.5 by addition of ammonia solution. The volume of the solution was made 120 mL by addition of distilled water followed by continuous stirring for 2 h. The solution was then transferred to a Teflon autoclave and treated hydrothermally at 160 °C for 15 h [22]. The precipitates were cooled down to room temperature and were thoroughly washed with distilled water and acetone. Finally, the obtained precipitates were dried in oven at 60 °C for 12 h.

#### 2.2.3. Synthesis of $MFe_2O_4$ via microemulsion approach

In this method, two separate emulsions (I and II) were prepared using water: SDS: hexane: 1-butanol in appropriate weight ratios [23]. Both the emulsions were allowed to stir for 10–15 min. Stoichiometric amounts of metal salts and ferric nitrate were added to emulsion (I) and aqueous solution of 5 M NaOH was added to emulsion II. After continuous stirring for 15 min, both the emulsions were mixed slowly followed by continuous stirring for 1 h at room temperature. The obtained precipitates were thoroughly washed followed by drying in oven at 60 °C for 12 h. The dried precipitates were then finally annealed in silica crucible for 5 h at 400 °C.

### 2.3. Physical techniques

To confirm the formation of M-O bonds, Fourier transform infrared (FT-IR) spectra were recorded using iS50-FT-IR instrument (Model no. AUP1200343). Powder X-ray diffraction (XRD) analysis was performed using Panalytical's X'pert Pro diffractometer with diffraction angles of 10–80° in increments of 0.02° to explore the structural properties. The morphology of the synthesized ferrites was observed using field emission scanning electron microscopy (FE-SEM) instrument (Hitachi-SU8010). High resolution transmission electron microscopy (HR-TEM) images of ferrite powders were obtained using FEI Tecnai (G2 F20) instrument operated at an accelerating voltage of 200 keV. The magnetic studies of the samples were done using vibrating sample

magnetometer (VSM) instrument Lake Shore 7400 with a magnetic field of  $\pm 10$  kOe at room temperature. The specific surface area of the samples was obtained by using Brunauer–Emmett–Teller (BET) surface area analyser ((11–2370) Gemini, Micromeritics, USA). Thin layer chromatography (TLC) was performed using pre-coated silica 60 F254, 0.25 mm aluminium plates (Merck) and the proceeding of reactions were visualized and studied under UV chamber. Confirmation of the formation of the desired product was scrutinized by using nuclear magnetic resonance (NMR) spectrometer (BRUKER AVANCE II 400 MHz) using TMS as an internal standard.

#### 2.4. Catalytic evaluation of the samples

The catalytic activity of all the synthesized spinel nanoferrites was evaluated for the aminolysis of the epoxides. The reactions were performed between equimolar amounts of epoxide and amine (1 mmol) using  $MFe_2O_4$  ( $M = Co, Ni, Cu$  and  $Zn$ ) nanoparticles as catalyst (10 mg), under solvent free conditions at  $80^\circ C$ . The progress of the reaction was monitored using thin layer chromatography (TLC). After the completion of reaction, the catalysts were magnetically separated from the reaction mixture and were thoroughly washed with distilled water and acetone to remove the organic or inorganic part. The recovered catalysts were then dried and recycled for further use. The final isolated products were analysed using  $^1H$  NMR, analysis and the obtained results were matched with those reported in literature [24].

### 3. Results and discussion

#### 3.1. Characterization

##### 3.1.1. FT-IR spectroscopy

FT-IR spectra for all the spinel nanoferrites ( $MFe_2O_4$ ;  $M = Co, Ni, Cu$  and  $Zn$ ) were recorded in the range of  $400\text{--}800\text{ cm}^{-1}$  and are shown in Fig. S1. It is well reported that the FT-IR spectra of ferrites exhibit two absorption bands corresponding to M-O bond stretching vibrations in tetrahedral and octahedral regions [25]. From Fig. S1, the absorption band in the range of  $500\text{--}600\text{ cm}^{-1}$  corresponding to M-O stretching vibrations of tetrahedral clusters for all the nanoferrites could be observed. However, the band corresponding to M-O stretching vibrations of octahedral clusters could not be observed which could be attributed to the peak shifting below  $400\text{ cm}^{-1}$  in case of octahedral M-O stretching vibrations [26].

##### 3.1.2. Powder XRD analysis

Structural characterization and phase identification of all the spinel nanoferrites ( $M = Co, Ni, Cu, Zn$ ) was appraised using XRD studies. The diffraction patterns of the prepared samples annealed at  $400^\circ C$  are given in the Fig. 1.

The crystallite size of all the ferrite compositions was calculated from the line broadening of the most intense peak (311) by using classical Scherrer equation [27,28].

$$D_{hkl} = 0.9\lambda/\beta\cos\theta \quad (1)$$

Where  $D_{hkl}$  is the crystallite size,  $\beta$  is the full width at half maxima,  $\lambda$  is the wavelength of the radiation used and  $\theta$  is the angle of diffraction. The crystallite sizes of all the samples prepared via different routes was found to be in the range of 6–26 nm and is listed in Table 1. The lattice parameter for all the metal ferrites prepared by different methods was calculated using Le Bail refinement method (built in TOPAS V2.1 of BRUKER AXS). The lattice parameter varies from 8.30 to 8.40 Å and the values are listed in Table 1.

##### 3.1.3. Structural analysis

The analysis of the shape and size of the presently investigated nanoferrite ( $MFe_2O_4$ ;  $M = Co, Ni, Cu$  and  $Zn$ ) synthesized using

different methods was done using FE-SEM. Typical FE-SEM images of  $CoFe_2O_4$  prepared by different routes are shown in Fig. 2. From the images, the homogenous nature of nanoferrites with small grain size distribution could be clearly observed. All the samples exhibited quasi-spherical shape with an average grain size of 14–20 nm  $CoFe_2O_4$  prepared by hydrothermal route was found to exhibit smallest grain size of 12–14 nm in comparison to  $CoFe_2O_4$  prepared via other routes.

HR-TEM studies were carried out for the further analysis of shape, size and purity of the obtained metal ferrites. Figs. 3(a), 4(a) and 5(a) show the low resolution TEM images of hydrothermally synthesized nanoparticles of  $CoFe_2O_4$ ,  $NiFe_2O_4$ , and  $ZnFe_2O_4$  respectively. From the images, the quasi spherical shape of the agglomerated nanoparticles with a size range of 12–20 nm could be clearly seen. Figs. 3(b), 4(b) and 5(b) show the HR-TEM images of the  $CoFe_2O_4$ ,  $NiFe_2O_4$ , and  $ZnFe_2O_4$  nanoparticles respectively. The interplanar distance values obtained from the HR-TEM images i.e 0.20 nm, 0.25 nm and 0.30 nm matched well with the corresponding XRD diffraction planes (4 0 0), (3 1 1) and (2 2 0) of  $CoFe_2O_4$ ,  $NiFe_2O_4$  and  $ZnFe_2O_4$  respectively.

The crystalline nature of the samples was depicted by concentric electron diffraction rings corresponding to different planes obtained in SAED patterns. Typical SAED (selected area electron diffraction) patterns of  $CoFe_2O_4$ ,  $NiFe_2O_4$  and  $ZnFe_2O_4$  nanoparticles synthesized by hydrothermal route are shown in Figs. 3(c), 4(c) and 5(c) respectively. The presence of the concentric diffraction rings illustrated the high crystalline nature of all the prepared spinel nanoferrites and all the planes observed from the SAED patterns matched well with the planes observed in the powder XRD patterns. The Energy Dispersive X-ray (EDX) spectra of  $CoFe_2O_4$ ,  $NiFe_2O_4$ , and  $ZnFe_2O_4$  nanoparticles synthesized by hydrothermal route are given in Figs. 3(d), 4(d) and 5(d) respectively. The results confirmed the existence of the constitutive elements Fe, Co, Zn, Ni and O in the synthesized samples. No superfluous peak was identified in the spectra which confirmed the purity of the prepared ferrite samples.

##### 3.1.4. Magnetic measurements

Magnetism is a fascinating phenomenon exhibited by materials and is allied with paired or unpaired electrons in the constituent atoms/ions in the material. The net magnetic moment of all the unpaired electrons in a material is responsible for the origin of interesting magnetic properties. The hysteresis loops of all the samples prepared by different routes were recorded using VSM in the magnetic range of  $\pm 10$  kOe. The hysteresis loops of all the metal ferrites are shown in Fig. 6. The saturation magnetization ( $M_s$ ), coercivity ( $H_c$ ), remanence ( $M_r$ ) and squareness ratio ( $S_q$ ) for all the nanoferrites synthesized by different methods are listed in Table 2.

The superparamagnetic nature in case of  $ZnFe_2O_4$  fabricated from all the three methods could be depicted from the hysteresis loops shown in Fig. 6 and low magnetization values given in Table 2. The saturation magnetization in the ferrites depends on the  $Fe^{3+}$  ion in A and B sites, which in turn depend upon the site preference of metal ion ( $M^{2+}$ ) in the lattice. As reported in literature,  $Zn^{2+}$  has tetrahedral site preference while the metal ions  $Co^{2+}$ ,  $Ni^{2+}$  and  $Cu^{2+}$  have octahedral site preference [29]. Therefore, in case of  $ZnFe_2O_4$ ,  $Fe^{3+}$  cations are present only in the B sites and thus it cannot undergo strong A-B super exchange interactions, which explains its super paramagnetic behaviour. Whereas, in case of  $CoFe_2O_4$ ,  $NiFe_2O_4$  and  $CuFe_2O_4$ , strong anti-ferromagnetic coupling between  $Fe^{3+}$  in A and B sites occurs resulting in high saturation magnetization values [30]. However, all the samples were found to be sufficiently magnetic to be employed as magnetically separable and recyclable heterogeneous catalysts.

##### 3.1.5. Specific surface area analysis

Keeping in mind the importance of surface area in catalysis, the specific surface area of the metal ferrite samples was calculated using BET surface area analyser. BET surface area basically collects the isotherm data obtained for the physical adsorption of an inert gas. For the

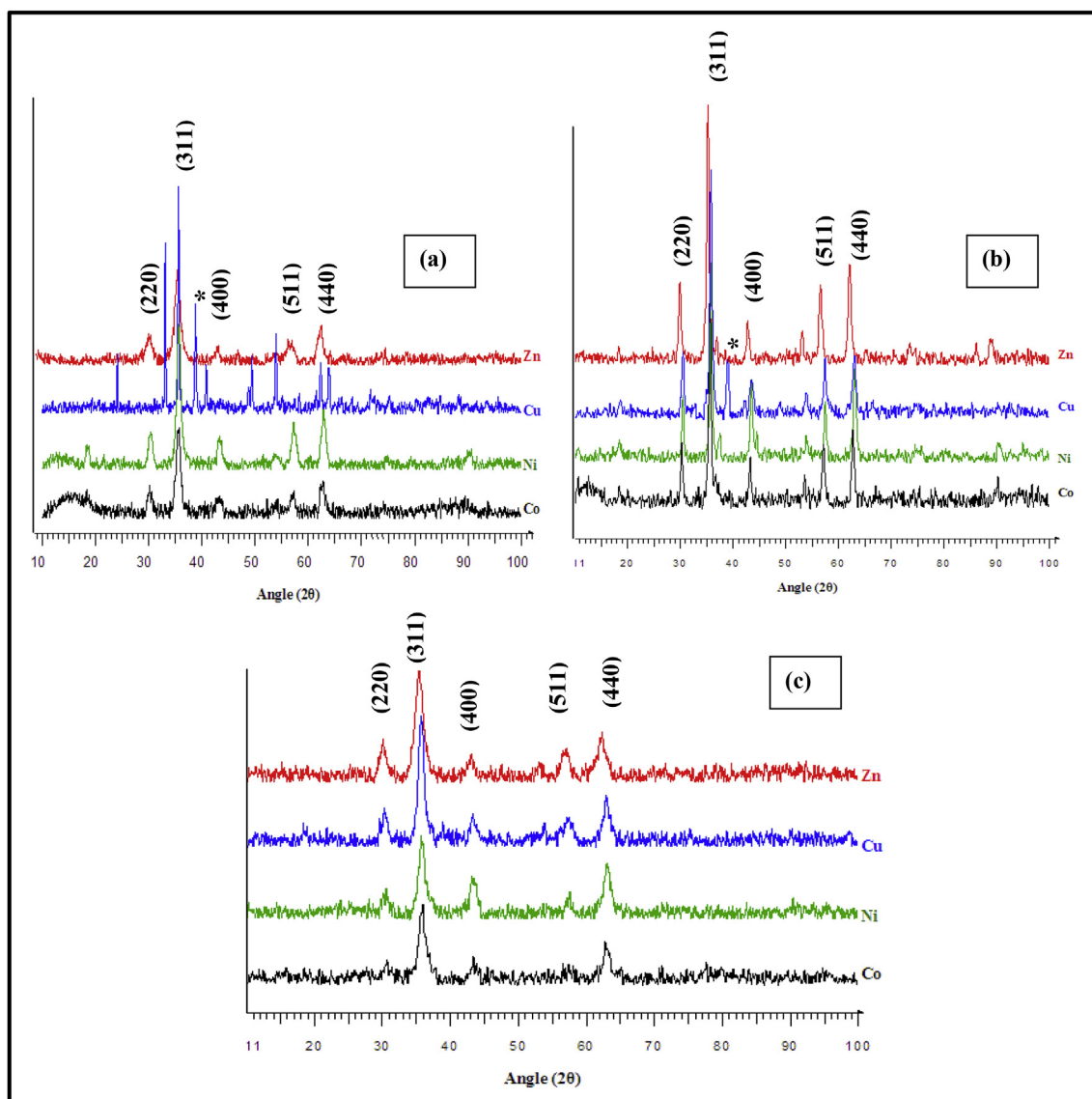


Fig. 1. Powder XRD patterns of  $MFe_2O_4$  ( $M = Co, Ni, Zn$  and  $Cu$ ) prepared by (a) hydrothermal method, (b) sol-gel method and (c) microemulsion method.

Table 1

Lattice parameter,  $a(\text{\AA})$  and Crystallite size  $D_{hkl}$  (nm) of the samples prepared by different method.

Method of preparation	Ferrites	$a$ ( $\text{\AA}$ )	$D_{hkl}$ $\pm 2$ (nm)
Hydrothermal	$CoFe_2O_4$	8.36	8
	$NiFe_2O_4$	8.33	26
	$ZnFe_2O_4$	8.40	26
	$CuFe_2O_4$	8.43	26
Sol-Gel	$CoFe_2O_4$	8.36	20
	$NiFe_2O_4$	8.33	26
	$ZnFe_2O_4$	8.40	17
	$CuFe_2O_4$	8.43	26
Microemulsion	$CoFe_2O_4$	8.36	6
	$NiFe_2O_4$	8.33	26
	$ZnFe_2O_4$	8.40	26
	$CuFe_2O_4$	8.43	5

current analysis, the samples were preheated at  $150^\circ\text{C}$  for 1 h before  $N_2$  absorption. The values of total surface area ( $S$ ) and specific surface area ( $S_{BET}$ ) were calculated using following equations [31].

$$S = Q_m N_S / V \quad (2)$$

$$S_{BET} = S / M \quad (3)$$

The specific surface areas of  $CoFe_2O_4$  samples synthesized using different techniques were obtained and all the samples were found to exhibit high specific surface area values. Maximum specific surface area value was obtained for  $CoFe_2O_4$  nanoparticles ( $1923.87 \text{ m}^2/\text{g}$ ) synthesized using hydrothermal method followed by microemulsion method ( $753.75 \text{ m}^2/\text{g}$ ) and sol-gel method ( $478.17 \text{ m}^2/\text{g}$ ). This trend in obtained specific surface area values was found to be in complete agreement with the trend in the particles size obtained from the FE-SEM (Fig. 2) and HR-TEM images (Figs. 3–5). The higher surface area values of all the nanoferrites indicated towards their potential use in the field of catalysis.

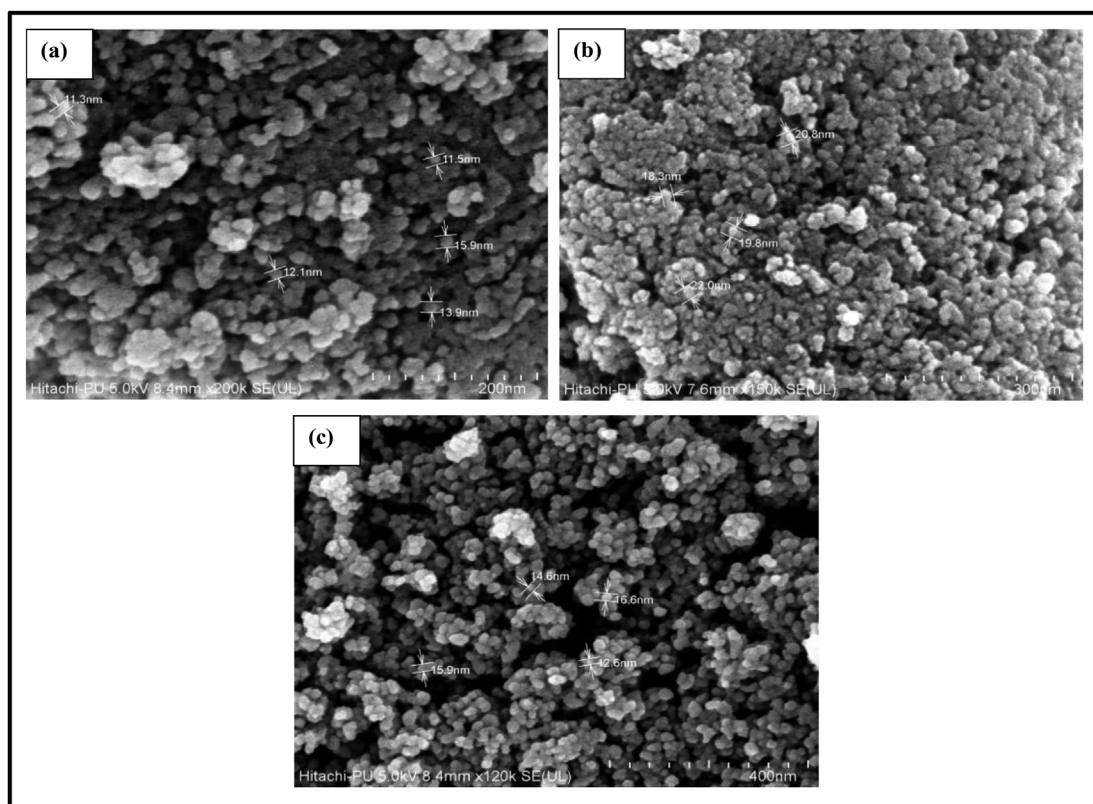


Fig. 2. FE-SEM images of  $\text{CoFe}_2\text{O}_4$  prepared by (a) hydrothermal technique, (b) sol-gel method and (c) microemulsion technique.

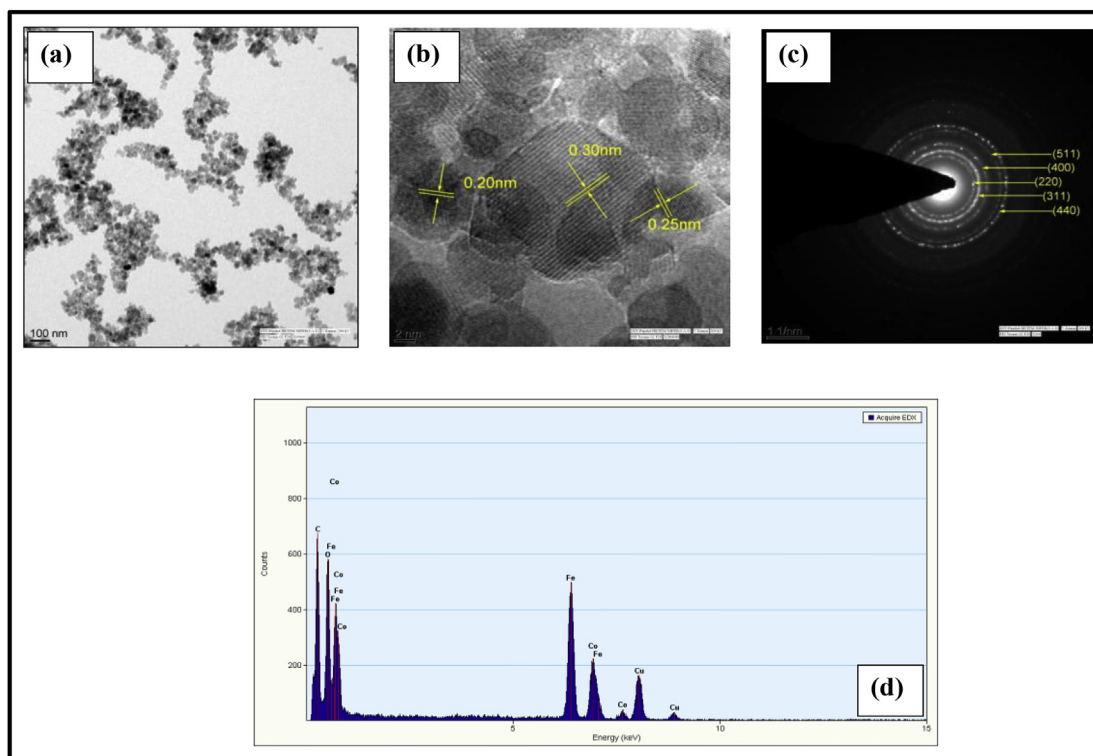


Fig. 3. Low Resolution TEM image (a), High Resolution TEM image (b), SAED pattern (c) and EDX (d) of  $\text{CoFe}_2\text{O}_4$  prepared by hydrothermal route.

### 3.2. Catalytic activity evaluation of $\text{MFe}_2\text{O}_4$ nanoparticles for epoxide ring opening reaction

All the reactions were chosen to be performed under solvent free

conditions to avoid the use of any toxic organic solvents. To find the best catalyst and its substrate scope, epoxides were allowed to react with various amines at  $80^\circ\text{C}$  in presence of different ferrites. Table 3 shows the catalyst optimization for the epoxide ring opening reaction of

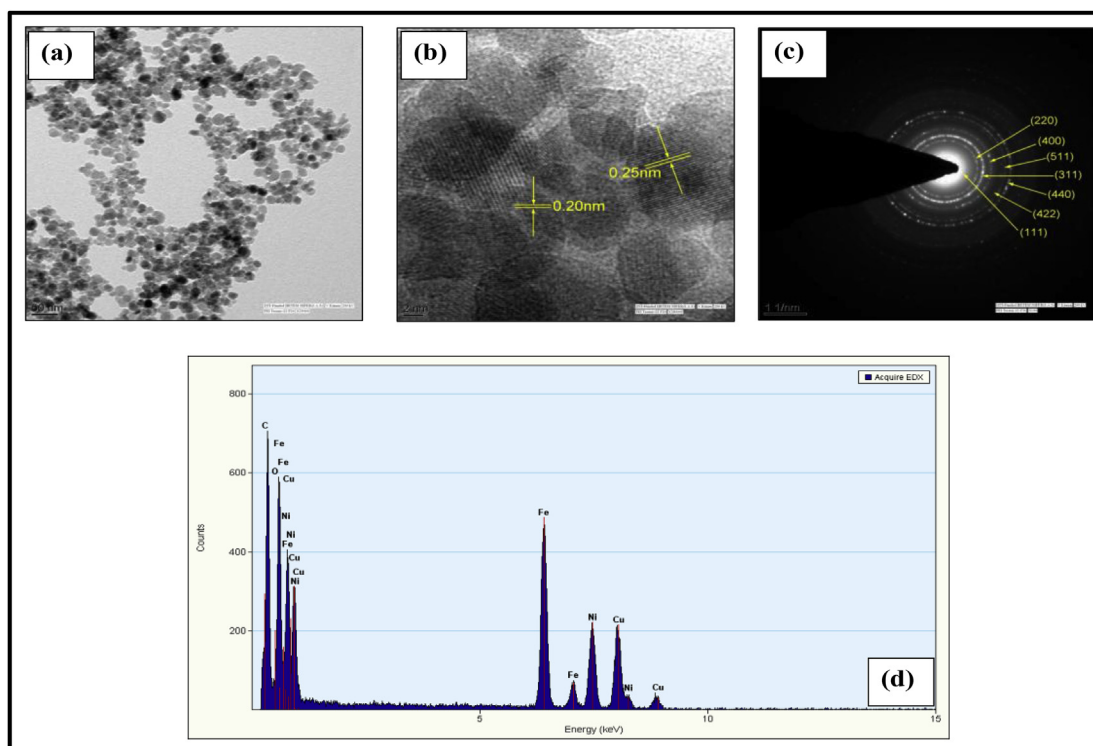


Fig. 4. Low Resolution TEM image (a), High Resolution TEM images(b), SAED pattern (c) and EDX (d) of  $\text{NiFe}_2\text{O}_4$  prepared by hydrothermal route.

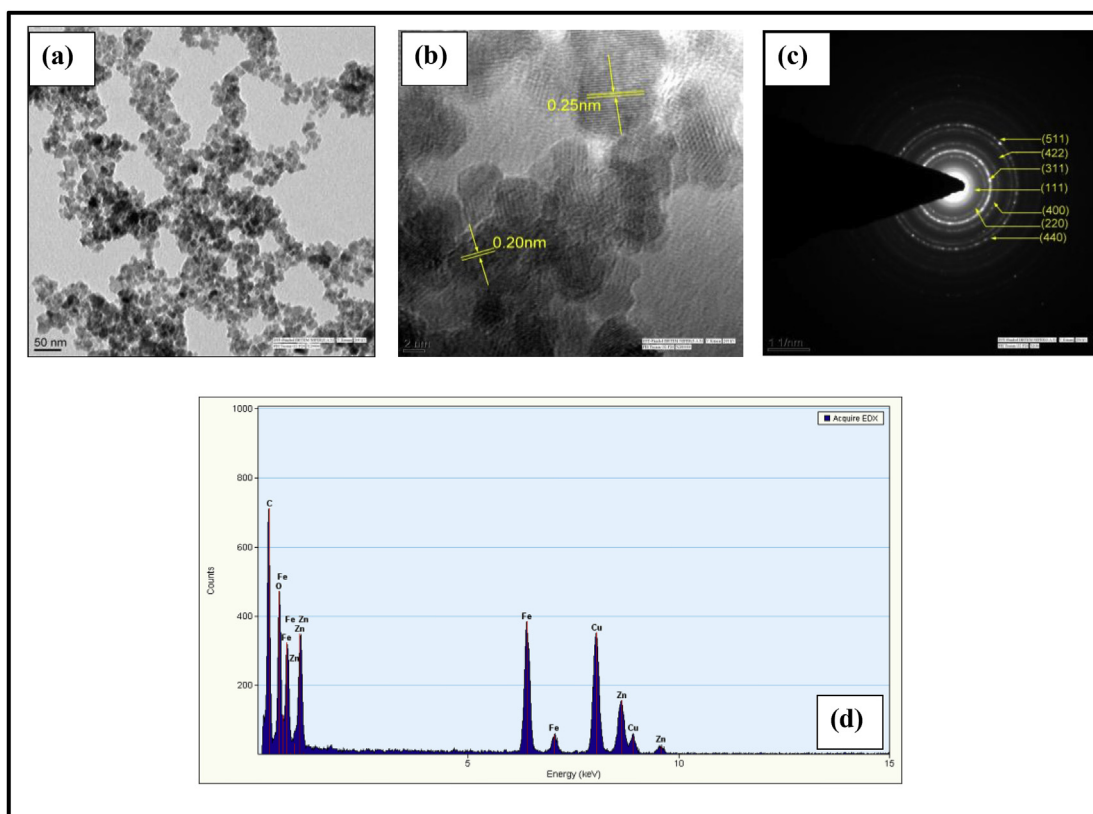


Fig. 5. Low Resolution TEM image (a), High Resolution TEM image (b), SAED pattern (c) and EDX (d) of  $\text{ZnFe}_2\text{O}_4$  prepared by hydrothermal route.

cyclohexene oxide (2) using aniline (1a) in the presence of all four spinel nanoferrites synthesized using different techniques. In all cases, only *trans* product i.e. *trans*-2-phenyl aminocyclohexanol (3a) was formed. The best results were obtained with  $\text{CoFe}_2\text{O}_4$  nanoparticles

synthesized by hydrothermal technique as it provided 100% conversion (GCMS) of reactants into corresponding amino alcohol within 5 min (Table 3, Entry 3). When,  $\text{CoFe}_2\text{O}_4$  nanoparticles synthesized by sol-gel method and micro-emulsion route were used as catalyst, conversion

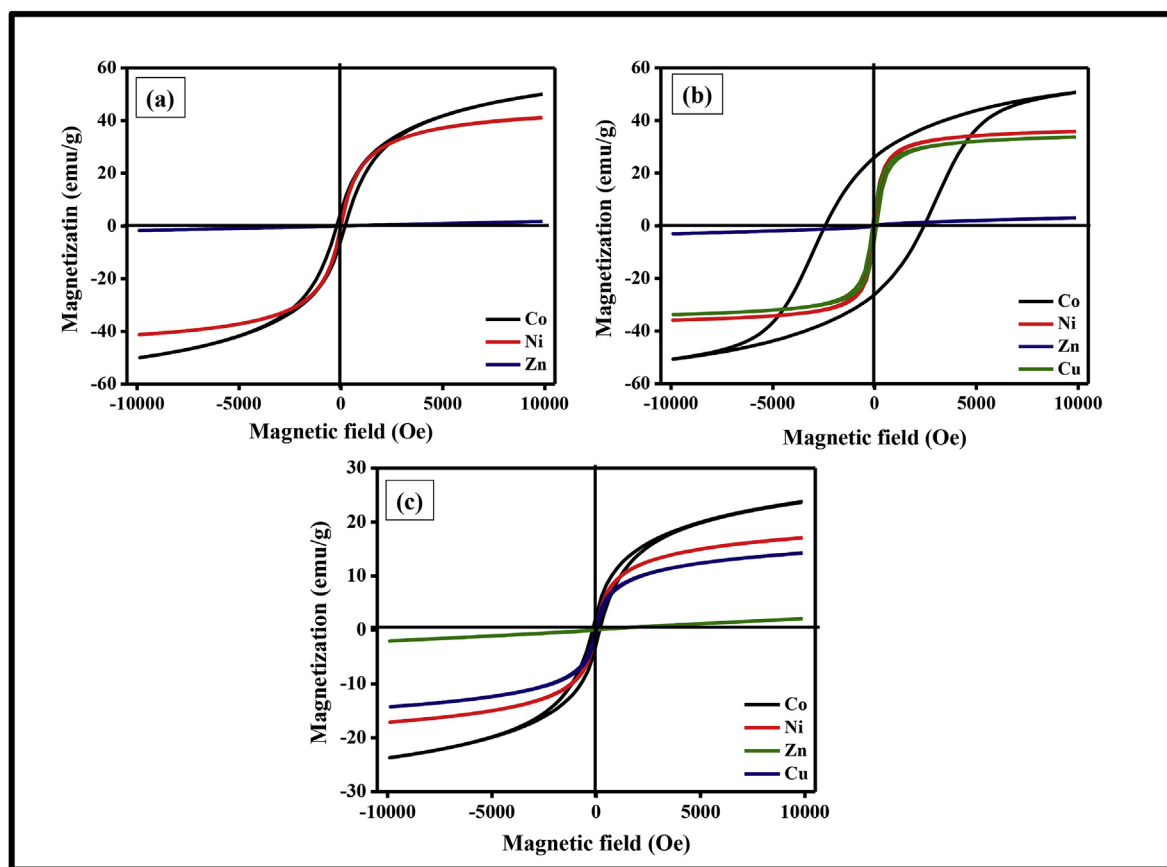


Fig. 6. Hysteresis loops of  $M\text{Fe}_2\text{O}_4$  ( $M = \text{Co}, \text{Ni}, \text{Zn}$  and  $\text{Cu}$ ) prepared by (a) hydrothermal route, (b) sol-gel route and (c) microemulsion route.

Table 2

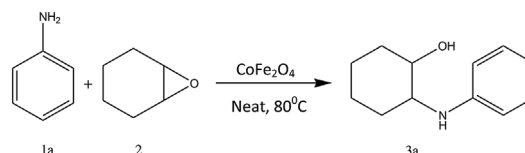
Remanence ( $M_r$ ), coercivity ( $H_c$ ), squareness ratio ( $S_q$ ), saturation magnetization ( $M_s$ ) of the samples prepared by different method.

Method of preparation	Ferrites	$M_r$ (emu/g)	$H_c$ (Oe)	$S_q \times 10^{-2}$	$M_s$ (emu/g)
Hydrothermal	$\text{CoFe}_2\text{O}_4$	3.8	308	7.7	50.0
	$\text{NiFe}_2\text{O}_4$	0.3	6	0.7	41.0
	$\text{ZnFe}_2\text{O}_4$	0	65	1.1	1.6
Sol-Gel	$\text{CoFe}_2\text{O}_4$	27.4	2400	54	50.7
	$\text{NiFe}_2\text{O}_4$	3.3	91	9.4	35.8
	$\text{CuFe}_2\text{O}_4$	5.3	92	15.7	33.6
Microemulsion	$\text{CoFe}_2\text{O}_4$	1.9	292	9.7	19.9
	$\text{NiFe}_2\text{O}_4$	0.3	17	1.7	17.0
	$\text{CuFe}_2\text{O}_4$	0.5	26	3.5	14.2

time was increased up to 8 and 10 min, respectively (Table 3, Entries 1 & 2). In case of  $\text{NiFe}_2\text{O}_4$  synthesized by sol-gel, micro-emulsion and hydrothermal route, 100% conversion was achieved in 30, 20 and 15 min, respectively (Table 3, Entries 4–6).  $\text{CuFe}_2\text{O}_4$  nanoparticles synthesized using sol-gel and micro-emulsion method provided 100% conversion in 20 min, while those synthesized using hydrothermal route resulted in 100% conversion in 50 min (Table 3, Entries 7–9).  $\text{ZnFe}_2\text{O}_4$  nanoparticles obtained from hydrothermal and microemulsion methods took 6 and 15 min for 100% conversion, respectively; while nanoparticles fabricated using sol-gel technique resulted in 100% conversion in 50 min (Table 3, Entries 10–12). This trend in the catalytic activity of different ferrites could be explained on the basis of smaller particle size of  $\text{CoFe}_2\text{O}_4$  nanoparticles synthesized using hydrothermal technique (FE-SEM and HR-TEM). As reported in literature, the catalytic activity of spinel nanoferrites is basically due to the octahedral

Table 3

$M\text{Fe}_2\text{O}_4$  catalyzed epoxide ring opening reaction with aromatic amine.



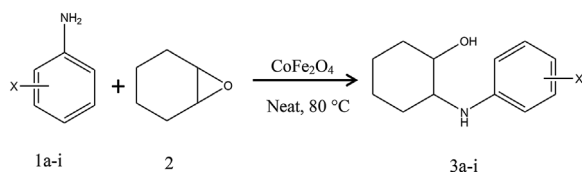
Entry	Catalyst	Synthetic method	Time (min)	% Conversion
1	$\text{CoFe}_2\text{O}_4$	Sol-gel	8	100
2	$\text{CoFe}_2\text{O}_4$	Microemulsion	10	100
3	$\text{CoFe}_2\text{O}_4$	Hydrothermal	5	100
4	$\text{NiFe}_2\text{O}_4$	Sol-gel	30	100
5	$\text{NiFe}_2\text{O}_4$	Microemulsion	20	100
6	$\text{NiFe}_2\text{O}_4$	Hydrothermal	15	100
7	$\text{CuFe}_2\text{O}_4$	Sol-gel	20	100
8	$\text{CuFe}_2\text{O}_4$	Microemulsion	20	100
9	$\text{CuFe}_2\text{O}_4$	Hydrothermal	60	100
10	$\text{ZnFe}_2\text{O}_4$	Sol-gel	50	100
11	$\text{ZnFe}_2\text{O}_4$	Microemulsion	15	100
12	$\text{ZnFe}_2\text{O}_4$	Hydrothermal	6	100

sites exposed on the surface.<sup>31</sup> The smaller particle size of the  $\text{CoFe}_2\text{O}_4$  nanoparticles resulted in the higher surface area (BET) and thus more catalytically exposed octahedral sites resulting in the better catalytic activity.

Next, the substrate scope of the  $\text{CoFe}_2\text{O}_4$  nanoparticles catalyzed methodology was evaluated by using different epoxides (2,4,6) with a variety of aromatic amines bearing electron withdrawing as well as electron donating groups (Tables 4–6). For all the reactions, excellent results were obtained with 100% conversion within 4–25 min to provide corresponding amino alcohols (NMR and GC-MS) in excellent

**Table 4**

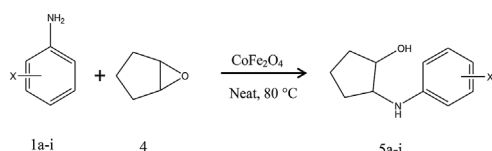
CoFe<sub>2</sub>O<sub>4</sub> (hydrothermal) catalyzed epoxide ring opening reaction with various aromatic amines.



Entry	Amine	Time (min)	Product	%Conversion	% Yield
1	X = H	5	X = H	100	92
2	X = 4-OMe	4	X = 4-OMe	100	93
3	X = 4-Me	4	X = 4-Me	100	92
4	X = 2-Cl	15	X = 2-Cl	100	85
5	X = 4-Cl	15	X = 4-Cl	100	85
6	X = 2-Br	12	X = 2-Br	100	90
7	X = 4-Br	12	X = 4-Br	100	89
8	X = 2-I	10	X = 2-I	100	89
9	X = 4-I	10	X = 4-I	100	88

**Table 5**

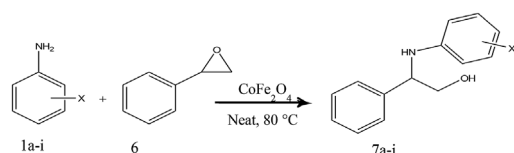
CoFe<sub>2</sub>O<sub>4</sub> (hydrothermal) catalyzed epoxide ring opening reaction with various aromatic amines.



Entry	Amine	Time (min)	Product	%Conversion	% Yield
1	X = H	5	X = H	100	92
2	X = 4-OMe	4	X = 4-OMe	100	92
3	X = 4-Me	4	X = 4-Me	100	93
4	X = 2-Cl	15	X = 2-Cl	100	90
5	X = 4-Cl	15	X = 4-Cl	100	88
6	X = 2-Br	12	X = 2-Br	100	89
7	X = 4-Br	12	X = 4-Br	100	89
8	X = 2-I	10	X = 2-I	100	88
9	X = 4-I	10	X = 4-I	100	88

**Table 6**

CoFe<sub>2</sub>O<sub>4</sub> (hydrothermal) catalyzed epoxide ring opening reaction with various aromatic amines.



Entry	Amine	Time (min)	Product	%Conversion	%Yield
1	X = H	10	X = H	100	89
2	X = 4-OMe	10	X = 4-OMe	100	90
3	X = 4-Me	10	X = 4-Me	100	88
4	X = 2-Cl	25	X = 2-Cl	100	82
5	X = 4-Cl	25	X = 4-Cl	100	82
6	X = 2-Br	20	X = 2-Br	100	84
7	X = 4-Br	20	X = 4-Br	100	84
8	X = 2-I	20	X = 2-I	100	82
9	X = 4-I	20	X = 4-I	100	83

isolated yields. For example: in case of *p*-OCH<sub>3</sub>, *p*-CH<sub>3</sub> anilines, reaction was very quick and corresponding products **3b** and **3c** were obtained within 4 min with 93% and 92% isolated yield, respectively. Halo-substituted anilines took little longer time to complete the reaction i.e.

10–15 min to provide the corresponding products in very high yields. Here it is noteworthy to mention that the reaction time was not affected by the position of halides on phenyl ring of aniline. For example: the reaction of 2-Br and 4-Br anilines with epoxides (**2**) consumed 12 min to give the products (**3f**) and (**3g**) in 90% and 89% yield, respectively. Same trend was observed in case chloro and iodo-substituted anilines also. In ring opening reaction of cyclopentanone epoxide (**4**) with *p*-OCH<sub>3</sub> and *p*-CH<sub>3</sub> aniline, the corresponding products were obtained in 92% and 93% isolated yield; respectively in 4 min. The reaction with halo-substituted anilines gave product in the range of 88–90% yield, with reaction time between 10 and 15 min. The longer time, in this case, was taken by chloro substituted anilines and as in case of epoxide (**2**) here also, the position of substituted halo groups does not affect the reaction time. Furthermore, the substrate scope was investigated by performing the reaction with unsymmetrical styrene epoxide (**6**). In this case, though the reaction time was little longer, 100% conversion was observed for each & every reaction as in case of symmetrical epoxides (**2**) & (**4**). For example when styrene epoxide (**6**) was allowed to react with anilines (**1a**), (**1b**), (**1c**) it provided the corresponding products (**6a**), (**6b**), (**6c**) in 89, 90 & 88% yield, respectively. Among the halo substituted anilines, chloro-aniline took 25 min for completion of reaction, while bromo and iodo-substituted aniline consumed 20 min for the 100% conversion. In all the cases, high yields were obtained for the corresponding products in the range of 80–84%.

To ensure the advantage of using ferrite nanoparticles in the aminolysis reaction, the reactions were performed under solvent free condition at 80 °C in the absence of any catalyst. The reaction resulted in only 18% conversion in 100 min confirming the application of current epoxide ring opening method. Also, it is the first ever study to investigate the method dependent comparative catalytic activity of magnetically recoverable spinel nanoferrites for the important epoxide ring opening reaction under solvent free conditions. To the best of our knowledge, no reports has been available in the literature where magnetically separable nanoferrites has been used as heterogeneous green catalysts for the epoxide ring opening reaction under solvent free conditions with 100% conversion in such short reaction times. The current work thus constitute an significant advance in the important field of epoxide ring opening reaction which could be well exploited in the synthesis of imperative organic compounds.

### 3.3. Characterization of product

The formation of all the desired products was confirmed and characterized using NMR spectroscopy. The <sup>1</sup>HNMR spectra and data of obtained product using CoFe<sub>2</sub>O<sub>4</sub> nanoferrite catalysts are given in supplementary information (Fig. S4-S30).

### 3.4. Plausible mechanistic pathway

It is well established that catalysis is a surface phenomenon and as reported earlier, the catalytic activity of spinel ferrites is mainly due to the metal ions present in the octahedral sites. When epoxide molecules get adsorbed onto the surface of ferrites, the acidic sites of ferrites get activated. The results obtained in Tables 3–6 could be rationalized on the basis of the mechanism given in Fig. 7. CoFe<sub>2</sub>O<sub>4</sub> nanoparticles exhibited better catalytic activity than other metal ferrites, which could be explained on the basis of stronger oxophilicity of Co<sup>2+</sup> ions as compare to Ni<sup>2+</sup>, Cu<sup>2+</sup> and Zn<sup>2+</sup> ions. The oxophilicity of ions basically depends on the acidic character of corresponding metal ions. Co<sup>2+</sup> ions exhibit highest total intrinsic acidity among the four ions and thus exhibited maximum catalytic activity [32].

On adsorption, one of the carbon atoms become electron deficient and so become facile for attack by the nucleophile. Hence the attack of nucleophile takes place on the electron deficient carbon atom of the epoxide resulting in the protonation of epoxide by the proton of the nucleophile. The results obtained in Tables 4 and 5 could be explained



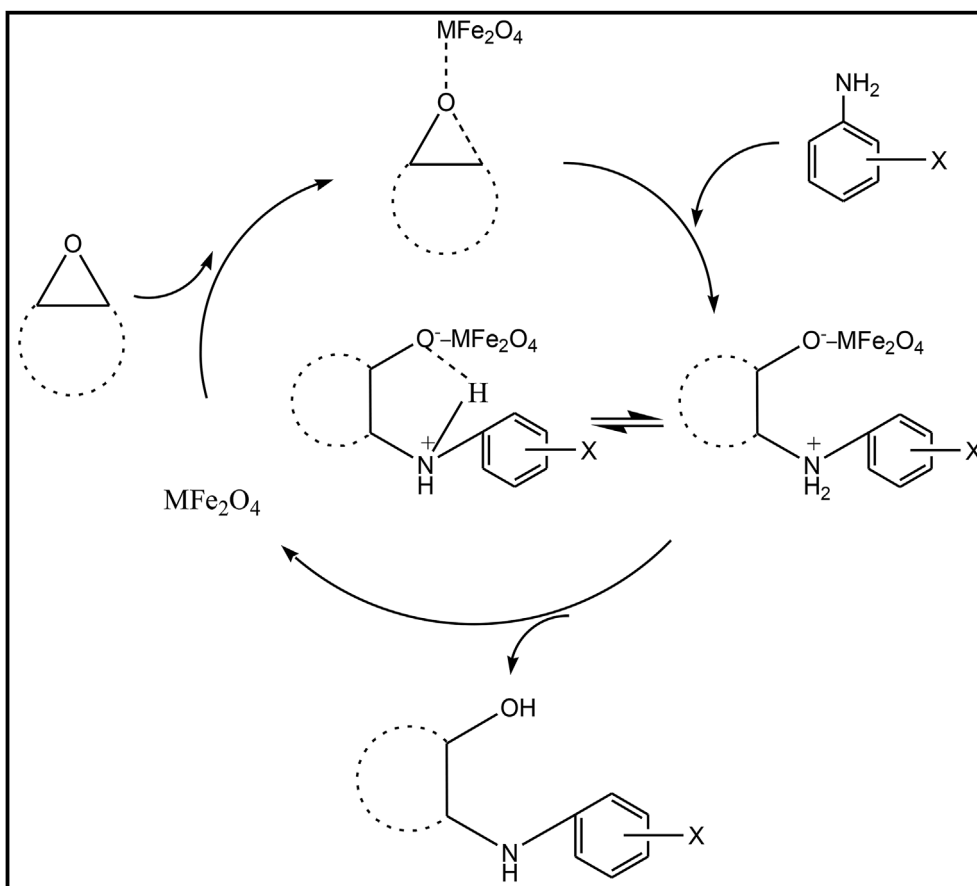


Fig. 7. Schematic representation of the reaction mechanism for the epoxide ring opening.

on the basis of nucleophilicity of different amines which follows the trend  $-\text{OMe} > -\text{Me} > \text{H} > \text{I} > \text{Br} > \text{Cl}$ . The higher nucleophilicity of  $-\text{OMe}$  substituted amine resulted in facile attack of nucleophile on the epoxide-ferrite complex resulting in the formation of final product *trans*-2-phenylaminocyclohexanol in lesser time.

### 3.5. Recyclability

Recyclability is one of the most important criteria in catalysis for the commencement of an economical and green reaction. Ferrites, being magnetic in nature, were easily separated using an external magnet and washed with distilled water and acetone. The obtained catalyst was then dried and used for further reactions. Fig. 8 shows the recyclability of  $\text{CoFe}_2\text{O}_4$  nanoparticles up to six cycles. As clear from the figure, no significant change in the catalytic activity of the ferrite sample was observed. The slight change obtained could be attributed to the loss of catalyst during washing and separation. The obtained results elucidated the advantage of using magnetically recoverable and recyclable spinel nanoferrites in the important epoxide ring opening reaction.

On completion of organic reactions, all the recovered catalysts were characterized using FT-IR and powder X-ray diffraction pattern. FT-IR spectra of nanoferrites showed absorption band in the range of  $500\text{--}600\text{ cm}^{-1}$  corresponding to M-O stretching vibrations of tetrahedral clusters and the typical FT-IR spectra of  $\text{CoFe}_2\text{O}_4$  prepared by hydrothermal route is given in Fig. S2. Also the XRD diffraction patterns of all recovered catalysts matched well with the diffraction planes (2 2 0), (3 1 1), (4 0 0), (5 1 1) and (4 4 0) of fresh catalysts and typical Powder XRD patterns of  $\text{CoFe}_2\text{O}_4$  prepared by hydrothermal route is given in Fig. S3. It was confirmed that there is no significant change in the recovered catalysts.

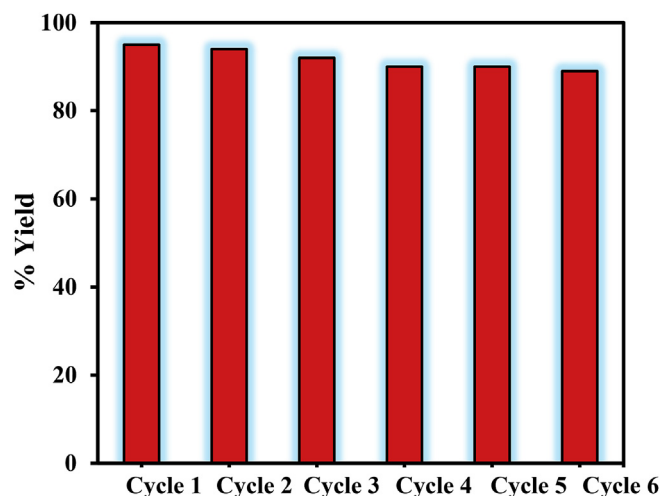


Fig. 8. Typical recyclability of hydrothermally prepared  $\text{CoFe}_2\text{O}_4$  nanoparticles for the ring opening of epoxide.

## 4. Conclusions

Magnetically separable spinel nanoferrites ( $\text{MFe}_2\text{O}_4$ ; M = Co, Ni, Cu and Zn) were successfully synthesized using different techniques viz. sol gel method, hydrothermal route and microemulsion technique. The spinel nanoferrites exhibited smaller particle size, large surface area, sufficiently magnetic nature and good recyclability and were found to be highly efficient as catalysts for epoxide ring opening reactions with amines under solvent free conditions.  $\text{CoFe}_2\text{O}_4$  nanoparticles prepared via hydrothermal route exhibited highest catalytic activity for the

conversion of different aromatic amines to corresponding amino alcohols with 100% conversion rate. The higher activity of  $\text{CoFe}_2\text{O}_4$  nanoparticles was associated with its smaller particle size, larger surface area and higher intrinsic acidity among the other metal ferrites. The current system thus exhibited a facile and solvent free greener approach using magnetically recyclable ferrites for the important epoxide ring opening reaction and thus could be potentially used as green catalysts for the formation of various pharmaceuticals and intermediate chemicals.

### Acknowledgements

The authors are highly thankful to CSIR (09/135(0783)/2017-EMR-1), DST-PURSE-II for providing necessary financial support and SAIF, Panjab University, Chandigarh for required sample characterizations.

### Appendix A. Supplementary data

Supplementary data to this article can be found online at <https://doi.org/10.1016/j.matchemphys.2018.10.021>.

### References

- [1] D. Celik, M. Yildiz, Investigation of hydrogen production methods in accordance with green chemistry principles, *Int. J. Hydrogen Energy* 42 (2017) 23395–23401.
- [2] D. Elhamifar, Z. Ramazani, M. Norouzi, R. Mirbagheri, Magnetic iron oxide/phenylsulfonic acid: a novel, efficient and recoverable nanocatalyst for green synthesis of tetrahydrobenzo[b] pyrans under ultrasonic conditions, *J. Colloid Interface Sci.* 511 (2018) 392–401.
- [3] J. Dantas, E. Leal, A.B. Mapossa, D.R. Cornejo, A.C.F.M. Costa, Magnetic nanocatalysts of  $\text{Ni}_{0.5}\text{Zn}_{0.5}\text{Fe}_2\text{O}_4$  doped with Cu and performance evaluation in transesterification reaction for biodiesel production, *Fuel* 191 (2017) 463–471.
- [4] I.T. Cunha, I.F. Teixeira, A.S. Albuquerque, J.D. Ardisson, W.A.A. Macedo, H.S. Oliveira, J.C. Tristão, K. Sapag, R.M. Lago, Catalytic oxidation of aqueous sulfide in the presence of ferrites ( $\text{MFe}_2\text{O}_4$ , M = Fe, Cu, Co), *Catal. Today* 259 (2015) 222–227.
- [5] H.M. Gobara, I.M. Nassar, A.M.A. El Naggar, G. Eshaq, Nanocrystalline spinel ferrite for an enriched production of hydrogen through a solar energy stimulated water splitting process, *Energy* 118 (2017) 1234–1242.
- [6] C. Luadthong, P. Khemthong, W. Nualpaeng, K. Faungnawakij, Copper ferrite spinel oxide catalysts for palm oil methanolysis, *Appl. Catal. A* 525 (2016) 68–75.
- [7] K. Jalaiah, K.V. Babu, Structural, magnetic and electrical properties of nickel doped Mn-Zn spinel ferrite synthesized by sol-gel method, *J. Magn. Magn. Mater.* 423 (2017) 275–280.
- [8] J.M. Kwon, J.H. Kim, S.H. Kang, C.J. Choic, J.A. Rajesha, K.S. Ahn, Facile hydrothermal synthesis of cubic spinel  $\text{AB}_2\text{O}_4$  type  $\text{MnFe}_2\text{O}_4$  nanocrystallites and their electrochemical performance, *Appl. Surf. Sci.* 413 (2017) 83–91.
- [9] P. Pulišová, J. Kováč, A. Voigt, P. Raschman, Structure and magnetic properties of Co and Ni nano-ferrites prepared by a two step direct microemulsions synthesis, *J. Magn. Magn. Mater.* 341 (2013) 93–99.
- [10] M. Sinha, S.K. Pradhan, Synthesis of nanocrystalline Cd–Zn ferrite by ball milling and its stability at elevated temperatures, *J. Alloy. Comp.* 489 (2010) 91–98.
- [11] F.M. Moghaddam, G. Tavakoli, F. Latifi, B. Saeednia,  $\alpha$ -Arylation of oxindoles using recyclable metal oxide ferrite nanoparticles: comparison between the catalytic activities of nickel, cobalt and copper ferrite nanoparticles, *Catal. Commun.* 75 (2016) 37–41.
- [12] S.V. Jadhav, K.M. Jinka, H.C. Bajaj, Nanosized sulfated zinc ferrite as catalyst for the synthesis of nopol and other fine chemicals, *Catal. Today* 198 (2012) 98–105.
- [13] S.A. Sarode, J.M. Bhojane, J.M. Nagarkar, An efficient magnetic copper ferrite nanoparticle: for one pot synthesis of 2-substituted benzoxazole via redox reactions, *Tetrahedron Lett.* 56 (2015) 206–210.
- [14] S.S. Shinde, M.S. Said, T.B. Surwase, P. Kumar, Mild regioselective and aminolysis of epoxides catalyzed by zirconium (IV) oxynitrate, *Tetrahedron Lett.* 56 (2015) 5916–5919.
- [15] Y.H. Liu, Q.S. Liu, Z.H. Zhang, Amberlyst-15 as a new and reusable catalyst for regioselective ring-opening reactions of epoxides to  $\beta$ -alkoxy alcohols, *J. Mol. Catal. Chem.* 296 (2008) 42–46.
- [16] N. Azizi, M.R. Saidi, Highly efficient ring opening reactions of epoxides with deactivated aromatic amines catalyzed by heteropoly acid in water, *Tetrahedron* 63 (2007) 888–891.
- [17] R.I. Kureshy, S. Singh, N.H. Khan, S.H.R. Abdi, E. Suresh, R.V. Jasra, Efficient method for opening of epoxides with amines by NaY zeolite under solvent-free conditions, *J. Mol. Catal. Chem.* 264 (2007) 162–169.
- [18] T. Ollevier, G.L. Compin, An efficient method for the ring opening of epoxides with aromatic amines catalyzed by bismuth trichloride, *Tetrahedron Lett.* 43 (2002) 7891–7893.
- [19] T. Baskaran, A. Joshi, G. Kamalakar, A. Sakthivel, A solvent free method for preparation of  $\alpha$ -amino alcohols by ring opening of epoxides with amines using MCM-22 as a catalyst, *Appl. Catal., A* 524 (2016) 50–55.
- [20] B. Sreedhar, P. Radhika, B. Neelima, N. Hebalkar, Regioselective ring opening of epoxides with amines using monodispersed silica nanoparticles in water, *J. Mol. Catal. Chem.* 272 (2007) 159–163.
- [21] S. Singhal, R. Sharma, T. Namgyal, S. Jauhar, S. Bhukal, J. Kaur, Structural, electrical and magnetic properties of  $\text{Co}_{0.5}\text{Zn}_{0.5}\text{Al}_x\text{Fe}_{2-x}\text{O}_4$  ( $x = 0, 0.2, 0.4, 0.6, 0.8$  and  $1.0$ ) prepared via sol-gel route, *Ceram. Int.* 38 (2012) 2773–2778.
- [22] M. Dhiman, R. Sharma, V. Kumar, S. Singhal, Morphology controlled hydrothermal synthesis and photocatalytic properties of  $\text{ZnFe}_2\text{O}_4$  nanostructures, *Ceram. Int.* 42 (2016) 12594–12605.
- [23] C. Singh, S. Jauhar, V. Kumar, J. Singh, S. Singhal, Synthesis of zinc substituted cobalt ferrite via reverse micelle technique involving in situ template formation: a study on their structural, magnetic, optical and catalytic properties, *Mater. Chem. Phys.* 156 (2015) 188–197.
- [24] J. Agarwal, A. Duley, R. Rani, R.K. Peddinti, Aminolysis of epoxides using iridium trichloride as an efficient catalyst, *J. Synth. Org. Chem.* 16 (2009) 2790–2796.
- [25] R. Ali, M.A. Khan, A. Manzoor, M. Shahid, M.F. Warsi, Structural and electro-magnetic characterization of Co-Mn doped Ni-Sn ferrites fabricated via micro-emulsion route, *J. Magn. Magn. Mater.* 441 (2017) 578–584.
- [26] Y. Koseoglu, F. Alan, M. Tan, R. Yilgin, M. Ozturk, Low temperature hydrothermal synthesis and characterization of Mn doped cobalt ferrite nanoparticles, *Ceram. Int.* 38 (2012) 3625–3634.
- [27] A. Goyal, S. Bansal, S. Singhal, Facile reduction of nitrophenols: comparative catalytic efficiency of  $\text{MFe}_2\text{O}_4$  (M = Ni, Cu, Zn) nano ferrites, *Int. J. Hydrogen Energy* 39 (2014) 4895–4908.
- [28] S. Jauhar, S. Singhal, Chromium and copper substituted lanthanum nano-ferrites: their synthesis, characterization and application studies, *J. Mol. Struct.* 1075 (2014) 534–541.
- [29] B.D. Cullity, Introduction to Magnetic Materials, Addison-Wesely Publishing Company Inc., Reading, MA, 1972.
- [30] S. Bhukal, Shivali, S. Singhal, Magnetically separable copper substituted cobalt-zinc nano-ferrite photocatalyst with enhanced photocatalytic activity, *Mater. Sci. Semicond. Process.* 26 (2014) 467–476.
- [31] A. Goyal, S. Kapoor, P. Samuel, V. Kumar, S. Singhal, Facile protocol for reduction of nitroarenes using magnetically recoverable  $\text{CoM}_{0.2}\text{Fe}_{1.8}\text{O}_4$  (M = Co, Ni, Cu and Zn) ferrite nanocatalysts, *RSC Adv.* 5 (63) (2015) 51347–51363.
- [32] C.G. Ramankutty, S. Sugunan, Surface properties and catalytic activity of ferros-pineles of nickel, cobalt and copper, prepared by soft chemical methods, *Appl. Catal. A* 218 (2001) 39–51.